

Polymer-Mediated Interaction between a Plate and a Sphere

Remco Tuinier,^{*,†} Gerrit A. Vliegenthart,[‡] and Henk N. W. Lekkerkerker[†]

Van't Hoff Laboratory, Debye Research Institute, University of Utrecht, Padualaan 8, 3584 CH Utrecht, The Netherlands, and School of Chemistry, University of Bristol, Cantock's Close, Bristol, BS8 1TS, United Kingdom

Received January 11, 2001; Revised Manuscript Received April 3, 2001

ABSTRACT: A recently developed method is applied to calculate the depletion interaction between a sphere and a flat plate due to nonadsorbing ideal polymers for arbitrary polymer–sphere ratios. The interaction potential is calculated from the polymer concentration profiles surrounding the sphere and plate based on the adsorption around the particles. The polymer concentration profile in the space near the two particles is the product of the polymer concentration profile due to the single plate and its profile around the single sphere. The product function profile is in good agreement with profiles calculated by computer simulations. The interaction potential derived from the adsorption using the product function agrees with analytical results for infinitely small and large spheres. It is shown that the force between a flat plate and a sphere goes to a minimum for large polymer–colloid ratios. These results show that a product function applies to the sphere–plate geometry and facilitates the calculation the depletion interaction between colloidal particles in complex cases.

1. Introduction

Asakura and Oosawa,¹ based on statistical mechanical results, showed that adding nonadsorbing ideal polymers to a colloidal dispersion induces attractions between the particles. A popular simplification of the depletion due to polymers is to replace the polymer concentration profiles around the particles by a step function, which is denoted as the penetrable hard-sphere (PHS) approach,^{2–4} where the diameter of the PHS has to be taken as $4R_g/\sqrt{\pi}$. Here R_g is the radius of gyration of an ideal polymer chain (for long chains $6R_g^2 \equiv b^2s$, where b is the segment length and s is the number of segments per chain). The PHS approach is, however, only successful in the limit $R \gg R_g$,^{5,6} where R is the sphere radius. For sphere/polymer size ratios where $R/R_g < 3$, the polymer concentration profile changes in both shape and range as a function of R/R_g .^{7–9} These effects can only be accounted for in a description of the interaction between particles if the polymer concentration profiles in the space surrounding the colloidal particles are known. For ideal chains the diffusion equation has to be elucidated. For simple geometries the diffusion equation may be calculated using Laplace transformations¹⁰ but become increasingly more difficult for more complex geometrical systems. To the authors' knowledge, exact solutions for two spheres in an ideal polymer solution have been found in the limit of $R/R_g \rightarrow \infty$ ¹¹ and $R/R_g \rightarrow 0$ ¹² but have not been found for arbitrary R/R_g values.

Recently, we have developed an approach to calculate the polymer concentration profiles between two particles by using the product function of the individual profiles.⁹ This Ansatz gives a good description of the profiles between two parallel plates and two spheres. In this paper the focus is on the interaction between a sphere and a plate immersed in an ideal polymer solution for arbitrary polymer–colloid size ratios. As a tool, we use the adsorption method^{13,14} which utilizes the polymer

concentration profiles to calculate the (negative) adsorption and hence the interaction between colloidal particles.

The significance of this study of the interaction between a sphere and a plate is twofold. First, it is a situation that can be validated experimentally. An example is atomic force microscopy (AFM), as performed by Milling and Biggs¹⁵ for studying polymer-induced depletion between a sphere and a surface. In this method one mounts a sphere onto the AFM cantilever which is then brought to the surface. The other method that allows a measurement accurate to $0.1kT$ is total internal reflection microscopy (TIRM).¹⁶ In this technique the particle–surface distance can be derived from the intensity of an evanescent wave that is formed when a photon beam is reflected from a surface at a sufficiently large incident angle. TIRM has been used by Walz and co-workers^{17–19} to study depletion interaction.

This study is also significant in that it facilitates the calculation of the interaction between a sphere and a plate, compared to the exact work that has been performed by Bringer et al.,²⁰ who derived various exact expressions under different conditions by solving the diffusion equation. We will summarize these results in section 2.2, which provide a good test for the applicability of our method to the interaction between a sphere and a plate and which could then be used to calculate the interaction potential curve for arbitrary polymer–colloid ratios. This would reduce the effort one has to put in by performing the quite complex numerical calculations.²⁰

2. Theoretical Section

We consider the situation depicted in Figure 1. A hard sphere with radius R is immersed in an ideal polymer solution, containing nonadsorbing polymers with a radius of gyration R_g . The (hard) sphere has a shortest distance h to a (hard) flat plate. Because of cylindrical symmetry, every point of the geometry is defined by x and z , as indicated in the figure. In this section we discuss two methods to calculate the interaction potential between a sphere and a plate as a function of h/R_g .

[†] University of Utrecht.

[‡] University of Bristol.

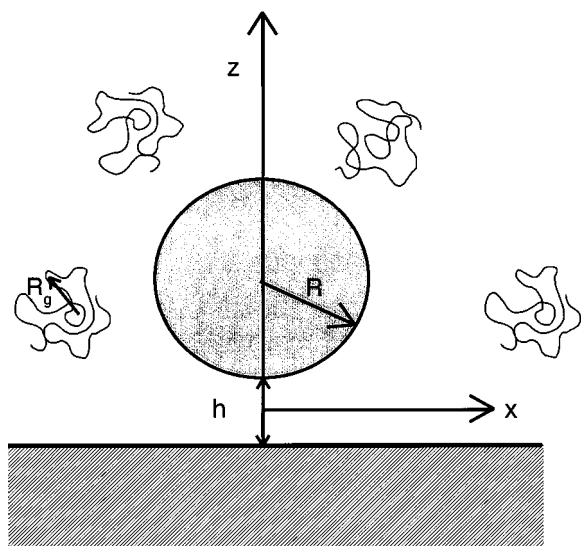


Figure 1. Schematic representation of the geometry of a sphere and plate in an ideal polymer solution separated by a distance h .

2.1. Adsorption Method. To calculate the interaction between a sphere and a plate in a nonadsorbing polymer solution, we use the extended Gibbs adsorption equation. The starting point is to define the grand potential Ω :

$$\Omega = F - \sum_i \mu_i N_i \quad (1)$$

where F is the Helmholtz free energy, μ_i is the chemical potential of component i , and N_i is the number of particles of that component in the system. An infinitesimal variation of Ω leads to the expression

$$d\Omega = -K dh - \sum_i N_i d\mu_i \quad (2)$$

at constant temperature and volume. In eq 2 h is the interparticle distance. For a system with nonadsorbing polymers and a background solvent only the chemical potential of the polymer molecules μ_p is significant. The interaction potential $W(h)$ is related to the force K by the equation

$$K = -\left(\frac{\partial W}{\partial h}\right)_{\mu_p} \quad (3)$$

so that the generalized Gibbs equation reads^{13,14}

$$-\left(\frac{\partial W(h)}{\partial \mu_p}\right)_h = N(h) - N(\infty) \quad (4)$$

which is derived from the substitution of eq 3 in eq 2, in which $N(h)$ is the amount of adsorbed polymer segments when the closest distance between the particles is h . The adsorption is the integral over the polymer segment concentration $n(r)$:

$$N(h) = \int_{V_p} dr [n(r) - n_b] \quad (5)$$

where V_p is the total volume of the polymer solution and n_b is the bulk polymer segment concentration.

For ideal chains eq 4 can be simplified to⁹

$$W(h) = -kT[N(h) - N(\infty)] \quad (6)$$

To determine the interaction potential between a sphere and a plate, the polymer concentration profile around a single sphere in the presence of the plate must be calculated. This can be achieved by applying the Ginzburg–Landau field theory.^{21–23} For ideal chains the excluded-volume interaction between the segments diminishes, meaning that the Edwards diffusion equation for polymers suffices:^{23,24}

$$\frac{\partial G_N(r, r')}{\partial N} = \frac{a^2}{6} \nabla_r^2 G_N(r, r') \quad (7)$$

with a boundary condition $G_0(r, r') = \delta(r - r')$. In eq 7 $G_N(r, r')$ is a Green function which describes the probability of finding the N th segment of the polymer chain at position r' while its origin lies at r . It is rather difficult to solve the differential equation (7) for a complex geometry, while there are solutions for a single wall and a single sphere, of which the significance will be shown later.

Eisenriegler²⁵ calculated the polymer concentration near one flat plate for ideal chains using Laplace transformations and found the following expression for the relative polymer concentration near a single plate $f_p(x) = n(x)/n_b$:

$$f_p(x) = 1 - 2 \left[(1 + 2z^2) \operatorname{erfc}(z) - \frac{2}{\sqrt{\pi}} z \exp(-z^2) \right] - \frac{4z}{\sqrt{\pi}} \exp(-4z^2) + (1 + 8z^2) \operatorname{erfc}(2z) \quad (8)$$

where z is defined as $x/(2R_g)$, and x is the distance from the surface.

Taniguchi et al.⁷ (see also ref 9) found the profile of ideal polymer chains around a single hard sphere $f_s(x)$ by solving eq 7 in spherical geometry. The result was

$$f_s(x) = \left(\frac{R}{R + 2zR_g} \right)^2 \left[\left(\frac{2zR_g}{R} \right)^2 + \left(\frac{zR_g}{R} \right) \left(\operatorname{erfc}(z) - 2z^2(1 - \operatorname{erfc}(z)) + \frac{2}{\sqrt{\pi}} z \exp(-z^2) \right) + 2 \operatorname{erfc}(z) - \operatorname{erfc}(2z) + \frac{4z}{\sqrt{\pi}} [\exp(-z^2) - \exp(-4z^2)] + 8z^2 \left[\frac{1}{2} - \operatorname{erfc}(2z) + \frac{1}{2} \operatorname{erfc}(z) \right] \right] \quad (9)$$

The profile around a sphere goes to $f_p(x)$ for $R \rightarrow \infty$. The range of the profile $f_s(x)$ decreases as R/R_g decreases and becomes independent of R_g for $R \rightarrow 0$. Our approximation is to take the product of the profiles as the local polymer segment concentrations, which follows from the superposition approximation that one may add two potentials that each generate a profile.⁹ In the situation schematically depicted in Figure 1, it is assumed that the local polymer concentration $n(r)$ at a certain point in the polymer solution, say P, defined by the vector r , is given by a product function:

$$\frac{n(r)}{n_b} = f_p(x_1) f_s(x_2) \quad (10)$$

where $f_p(x_1)$ and $f_s(x_2)$ are the relative polymer concen-

trations given by eq 8 (with $x = x_1$) and eq 9 (with $x = x_2$, being the nearest distance from the surface of the sphere to position P), respectively. The combination of eqs 5, 6, and 8–10 yields the interaction potential between a sphere and a plate as a function of the closest sphere plate distance h .

2.2. Limiting Functions from Diffusion Equation. Bringer et al.²⁰ derived analytical expressions for the interaction between a plate and a sphere by solving the diffusion equation within specific limits. For ideal chains they obtained the general expression

$$\frac{W(h)}{kT\phi_p} = -\frac{R}{R_g} Y\left(\frac{h}{R_g}, \frac{R}{R_g}\right) \quad (11)$$

where the relative polymer concentration ϕ_p equals $4\pi n_b R_g^3/3s$, and Y is a scaling function that depends on h/R_g and R/R_g . The scaling function can be precisely calculated in two limits. For spheres that are very small relative to the polymer chains the s segments treat the sphere as a pointlike object that gives a weak repulsive potential.²¹ For a sphere that is very close to the wall ($h \ll R_g$) this leads to²⁰

$$Y^{\text{small}}\left(\frac{h}{R_g}\right) = \frac{3}{2}\left[1 - \left(\frac{h}{R_g}\right)^2\right] \quad (12)$$

while for spheres that are very large relative to the polymer size one can apply the Derjaguin approximation²⁶ to the result of two parallel plates.¹¹ For $h \ll R_g$ this leads to the scaling function:^{11,20}

$$Y^{\text{large}}\left(\frac{h}{R_g}\right) = 3 \ln(2) - \frac{3}{\sqrt{\pi}}\left(\frac{h}{R_g}\right) + \frac{3}{8}\left(\frac{h}{R_g}\right)^2 \quad (13)$$

For very large separations between the wall and the sphere the scaling function becomes independent of R/R_g and reads²⁰

$$Y\left(\frac{h}{R_g}\right) = \frac{24}{\sqrt{\pi}}\left(\frac{h}{R_g}\right)^{-3} \exp\left(-\frac{1}{4}\left(\frac{h}{R_g}\right)^2\right) \quad (14)$$

We will compare our method described in section 2.1 for the interaction potential with eq 11 using the exact analytical expressions for the scaling function given by eqs 12–14. This is an excellent test for the validity of our approximation described in section 2.1.

3. Results and Discussion

Representative results for the local polymer concentration profiles for $R = R_g$ are presented in Figure 2 for $h/R_g = 0$ (a), $h/R_g = 0.25$ (b), and $h/R_g = 2.45$ (c). Equation 10 is plotted in the figures as the curves as a function of z for various values of x as indicated. The symbols represent computer simulations that were obtained by placing random walks of 100 segments in a box containing a sphere and a flat plate. Those random walks that crossed an interface or are inside the sphere are assigned a zero weight. All other configurations are weighted with equal probability. As shown, results from eq 10 are in close agreement with the data derived from computer simulations. At this level eq 10 leads to a good description of the local polymer concentration profiles.

Since the product function (eq 10) describes the local polymer concentration profiles quite well, the profiles

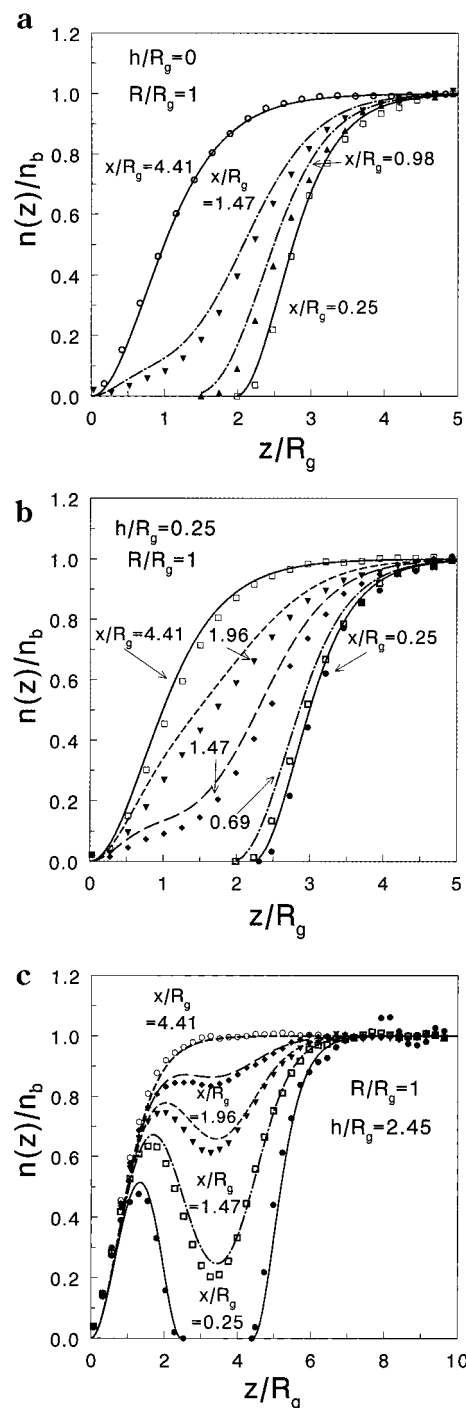


Figure 2. (a) Polymer concentration profiles in the region around a sphere close to a plate for $R/R_g = 1$, $h = 0$, and $x/R_g = 0.06, 0.24, 0.36$, and 1.1 . The symbols are the computer simulation results. The curves correspond to the product function Ansatz. (b) As in (a) for $h/R_g = 0.25$ and $x/R_g = 0.06, 0.17, 0.36, 0.48$, and 1.1 . (c) As in (a) for $h/R_g = 2.45$ and $x/R_g = 0.06, 0.36, 0.48$, and 1.08 .

were inserted into eq 5, and the interaction potential between a sphere and a plate was calculated using eq 6. In Figure 3 the interaction potential is plotted as a function of h/R_g for four values of q ($\equiv R/R_g$): 10, 1, 0.1, and 0.01. The potentials $W(h)$ (dashed curves) are normalized by $q\phi_p kT$. Since $-W(h)/q\phi_p kT = Y(h/R_g)$, effectively the scaling function $Y(h/R_g)$ was plotted as a function of h/R_g (see eq 11). Where $h/R_g > 2$, it was found that the scaling function is independent of q . This corresponds to eq 14, the scaling function of Bringer et

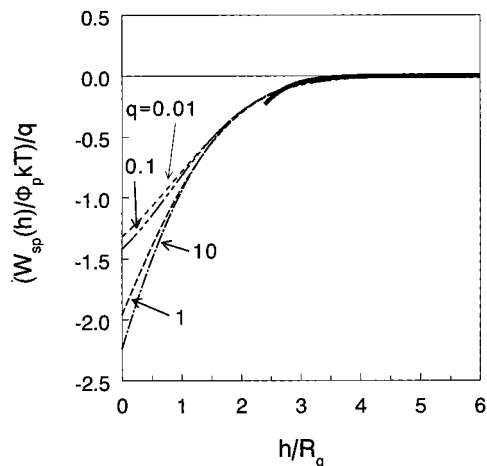


Figure 3. Normalized interaction potential between a sphere and a plate immersed in an ideal polymer solution for $R/R_g = 10, 1, 0.1$, and 0.01 . The dashed curves are the result from the adsorption method using the product function. The solid curve is the exact result for $h \gg R_g$ (eq 14).

al.,²⁰ which is independent of q for very large h . Equation 14 is plotted as the solid curve in Figure 3. For small h/R_g values differences in the shape of the scaling functions as a function of q were found. The absolute value of the minimum of the potential decreases with decreasing q , and for $q = 0.1$ and 0.01 an inflection point is observed which is not present for $q = 1$ and 10 .

In Figure 4a–c we check whether the interaction potentials calculated from the product function agree with the exact results for very small h/R_g . In Figure 4a, where $q = 10$, it is observed that the exact result for the limiting scaling function (solid curve) for small h , calculated from eq 13, is consistent with the results that are derived from eqs 10, 5, and 6 and also seems to scale analogously for small h/R_g . Where $q = 1$ (Figure 4b) the scaling function of eq 13 also gives a good description of the interaction potential for small h , although it is definitely not in the infinitely large radius regime at this stage. The scaling function for small spheres (eq 12) differs much more from our result for $q = 1$. For $q = 0.1$ (Figure 4c) and 0.01 (not shown) the scaling function for the small spheres (eq 12) is well described by the adsorption method using eq 10.

By applying eq 3, the force was calculated from the interaction potential. Exact results for the force are also available as is shown below. A comparison of the exact result for the force with the data derived from eq 10 is a sensitive test for the product function with exact results since small quantitative differences are enlarged by differentiation (see eq 3). Results for the force between sphere and plate are plotted in Figure 5. The results from the product function are given by the dashed curves. Surprisingly, there appears to be a minimum in the force as a function of h for $q = 0.01$ and 0.10 . The minimum lies near $h/R_g = 0.8$ and can be understood qualitatively by replacing the depletion layers with a step function (see also the schematic picture of Figure 6). The depletion layer due to a single hard plate has a width of approximately R_g , denoted by ξ_p in Figure 6. Around a very small sphere the depletion layer is close to $3R$, as indicated by ξ_s . So, for relatively large polymer chains the depletion layer around the sphere (ξ_s) is negligible compared to that near the single wall (ξ_p). When the small sphere, including a depletion

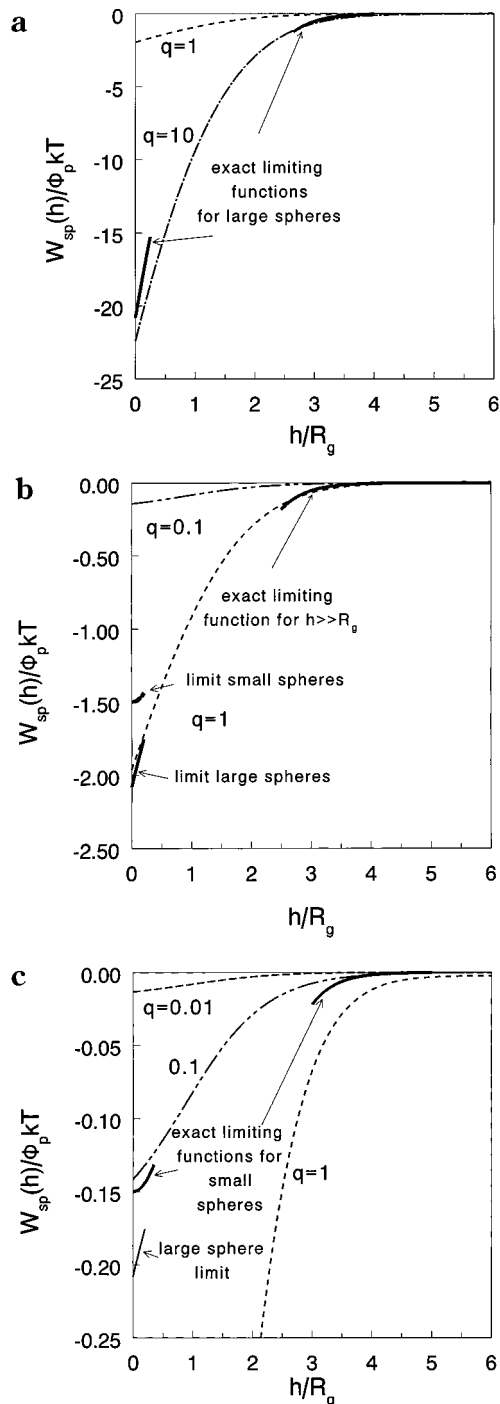


Figure 4. (a) Interaction potential for $R/R_g = 10$ calculated from the adsorption method using the product function (dashed curve) compared with the exact results of eq 11 (solid curve), with eqs 13 and 14 in the limit of $h \rightarrow 0$ for large spheres and $h \gg R_g$, respectively. (b) As in (a) but for $R/R_g = 1$, compared with the exact results of eq 11 with eqs 13, 12, and 14 in the limit of $h \rightarrow 0$ (for large and small spheres) and $h \gg R_g$, respectively. (c) As in (a) but for $R/R_g = 0.1$ compared with the exact results of eq 11 with eqs 13, 12, and 14 in the limit of $h \rightarrow 0$ (for large and small spheres) and $h \gg R_g$, respectively.

layer $\xi_s (\ll \xi_p)$, is located inside the depletion layer (ξ_p) of the wall, the overlap volume of depletion layers does not increase further when the sphere is moved toward the wall. Just replacing the profiles by effective depletion layers would mean that the interaction potential (osmotic pressure times overlap volume) has a minimum value if h is smaller than approximately $(\xi_p - 5R)$ and does not decrease when the sphere is pushed further

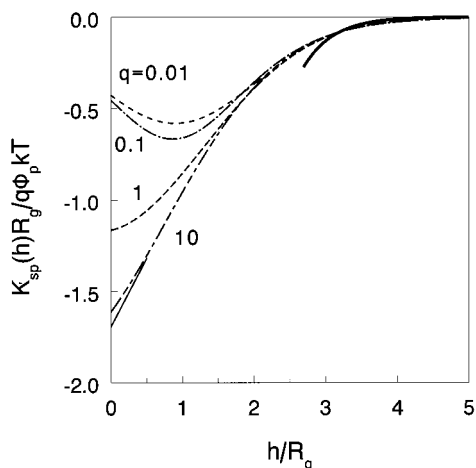


Figure 5. Force between a wall and a sphere for $R/R_g = 0.01, 0.1, 1,$ and $10,$ calculated from the adsorption method using the product function (dashed curves). The curves are compared with the exact results of eq 15 (solid curves), using expressions 18 and 19 in the limit of $h \rightarrow 0$ for large spheres and for $h \gg R_g,$ respectively.

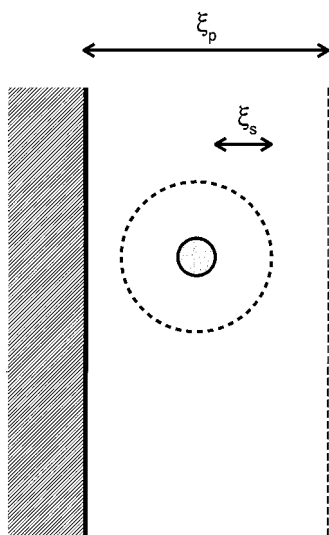


Figure 6. Schematic picture of the situation that a small sphere enters the depletion layer near a plate. The depletion layer due to the plate is indicated by $\xi_p.$ The depletion layer around the single sphere is given by $\xi_s.$

toward the plate. This would lead to a diminishing force at contact, which is only found for infinitely small spheres. In the product function Ansatz this effect is accounted for since it is observed that the normalized force increases with decreasing relative sphere size. It would be very interesting to observe this phenomenon experimentally.

Our results can be compared with analytical results in two limits, given by the solid curves. By applying eq 3, eq 11 becomes

$$\frac{K(h)}{kT\phi_p} = \frac{R}{R_g^2} Q\left(\frac{h}{R_g}, \frac{R}{R_g}\right) \quad (15)$$

In eq 15 the scaling function Q follows from differentiation of the scaling function Y : $Q = -\partial Y/\partial(h/R_g).$ From eq 12 it then follows that $Q = 0$ at $h = 0$ for infinitely small spheres, corroborating the concept outlined above. For infinitely small spheres the scaling function Y in

eq 11 reads²⁰

$$Y^{\text{small}}\left(\frac{h}{R_g}\right) = \frac{3\pi^{1/2}}{2\Gamma\left(\frac{1}{2}\right)} [f_p(h) - 1] \quad (16)$$

where $f_p(h)$ is given by eq 8 with x replaced by $h.$ Upon differentiation the following expression for Q is obtained:

$$Q^{\text{small}}\left(\frac{h}{R_g}\right) = -\frac{6}{\Gamma\left(\frac{1}{2}\right)} \left[\exp\left(-\left\{\frac{h}{2R_g}\right\}^2\right) - \exp\left(-4\left\{\frac{h}{2R_g}\right\}^2\right) + \frac{h}{R_g} \sqrt{\pi} \operatorname{erf}\left(\frac{h}{R_g}\right) + \frac{h}{2R_g} \sqrt{\pi} \operatorname{erf}\left(\frac{h}{2R_g}\right) \right] \quad (17)$$

which has a minimum value h_{\min} at $16 \operatorname{erf}(h_{\min}/R_g) - 8 \operatorname{erf}(h_{\min}/2R_g) = 8,$ so $h_{\min} \approx 0.72R_g.$ This is in reasonable agreement with our finding using the product function, $h_{\min} \approx 0.8R_g.$ The minimum value of Q of eq 17 is close to $-0.97,$ whereas our result gives a value of $-0.58.$ This shows that there is a significant difference in the limit of extremely small spheres. The product function is obviously less accurate in that limit. From eq 13 we obtain the following limit for very large ($R \gg R_g$) spheres for $h \ll R_g:$

$$Q^{\text{large}}\left(\frac{h}{R_g}\right) = -\frac{3}{\sqrt{\pi}} + \frac{3}{4}\left(\frac{h}{R_g}\right) \quad (18)$$

which is plotted in Figure 5 as the solid curve. Where $R/R_g = 10,$ the data agree very well with this expression. The force at contact determined in the current study is $-1.61q\phi_p kT,$ which is in close agreement with the contact force as determined from eq 18: $-3q\phi_p kT/\sqrt{\pi} \approx -1.69q\phi_p kT.$ For very large h/R_g values we find from eq 14

$$Q\left(\frac{h}{R_g}\right) = -\frac{12}{\sqrt{\pi}} \left(\frac{h}{R_g}\right)^{-4} \exp\left(-\frac{1}{4}\left(\frac{h}{R_g}\right)^2\right) \left[\left(\frac{h}{R_g}\right)^2 + 6\right] \quad (19)$$

which is also plotted in Figure 5. The curves calculated with our Ansatz correspond well with eq 19 for large $h/R_g.$ Both for the force and for the potential the results collapse onto a single curve for $h \gg R_g.$

4. Conclusions

Using a product function Ansatz, the polymer concentration profiles between a sphere and a plate were determined. The values obtained agree with the results for the local polymer segment concentration from our method, as compared with a random walk computer simulation. By integrating the profiles, the negative adsorption as a function of the distance between the plate and the sphere was calculated. For both small and large $h/R_g,$ where h is the closest sphere–plate distance and R_g is the radius of gyration, the results agree reasonably well with exact analytical expressions derived from the diffusion equation. These analytical expressions are available both in the limit of $R \gg R_g,$ where R is the sphere radius, as well as for $R_g \gg R.$ By differentiation, we calculate the force between the two objects, which shows that the force goes through a minimum as a function of $h.$ Thus, except for spheres that are much smaller than the polymer chains, the

product function gives good quantitative results for the interaction potential and for the force between a plate and a sphere in an ideal polymer solution.

Acknowledgment. R.T. thanks E. Eisenriegler and A. Bringer, Forzungscentrum Jülich, Germany, for useful and pleasant discussions on plate–sphere interactions. We acknowledge J. Groenewold, Van't Hoff Laboratory, University of Utrecht, for useful discussions. We are indebted to J. O'Connell, NIZO food research, for a critical reading of the manuscript. An anonymous reviewer is thanked for the suggestion to compare our results for the force for very small spheres with eq 17. The NWO-Unilever program financially supported this work.

References and Notes

- (1) Asakura, S.; Oosawa, F. *J. Chem. Phys.* **1954**, *22*, 1255.
- (2) Vrij, A. *Pure Appl. Chem.* **1976**, *48*, 471.
- (3) Gast, A. P.; Hall, C. K.; Russel, W. B. *J. Colloid Interface Sci.* **1983**, *96*, 251.
- (4) Lekkerkerker, H. N. W.; Poon, W. C. K.; Pusey, P. N.; Stroobants, A.; Warren, P. B. *Europhys. Lett.* **1992**, *20*, 559.
- (5) Meijer, E. J.; Frenkel, D. *J. Chem. Phys.* **1994**, *100*, 6873.
- (6) Dijkstra, M.; Brader, J. M.; Evans, R. *J. Phys: Condens. Matter* **1999**, *11*, 10079.
- (7) Taniguchi, T.; Kawakatsu, T.; Kawasaki, K. *Slow Dyn. Condens. Matter* **1992**, *256*, 503.
- (8) Eisenriegler, E.; Hanke, A.; Dietrich, S. *Phys. Rev. E* **1996**, *54*, 1134.
- (9) Tuinier, R.; Vliegthart, G. A.; Lekkerkerker, H. N. W. *J. Chem. Phys.* **2000**, *113*, 10768.
- (10) Eisenriegler, E. *Polymer near Surfaces*; World Scientific: Singapore, 1993.
- (11) Eisenriegler, E. *Phys. Rev. E* **1997**, *55*, 3116.
- (12) Eisenriegler, E. *J. Phys: Condens. Matter* **2000**, *12*, A227.
- (13) Hall, D. G. *J. Chem. Soc., Faraday Trans.* **1972**, *68*, 2169.
- (14) Ash, S. G.; Everett, D. H.; Radke, C. *J. Chem. Soc., Faraday Trans.* **1973**, *69*, 1256.
- (15) Milling, A.; Biggs, S. *J. Colloid Interface Sci.* **1995**, *170*, 604.
- (16) Prieve, D. C.; Frej, N. A. *Langmuir* **1990**, *6*, 396.
- (17) Sober, D. L.; Walz, J. Y. *Langmuir* **1995**, *11*, 2352.
- (18) Sharma, A.; Walz, J. Y. *J. Chem. Soc., Faraday Trans.* **1996**, *92*, 4997.
- (19) Sharma, A.; Walz, J. Y. *J. Colloid Interface Sci.* **1997**, *191*, 236.
- (20) Bringer, A.; Eisenriegler, E.; Schlesener, F.; Hanke, A. *Eur. Phys. J. B* **1999**, *11*, 101.
- (21) Eisenriegler, E. In *Field Theoretical Tools in Polymer- and Particle-Physics*; Meyer-Ortmanns, H., Klümper, A., Eds.; Lecture Notes in Physics No. 508; Springer: Berlin, 1998.
- (22) Schäfer, L. *Excluded Volume Effects in Polymer Solutions*; Springer: Heidelberg, 1999.
- (23) De Gennes, P. G. *Scaling Concepts in Polymer Physics*; Cornell University Press: Ithaca, NY, 1979.
- (24) Doi, M.; Edwards, S. F. *The Theory of Polymer Dynamics*; Clarendon Press: New York, 1986.
- (25) Eisenriegler, E. *J. Chem. Phys.* **1983**, *79*, 1052.
- (26) Deryaguin, B. V. *Kolloid Z.* **1934**, *69*, 155.

MA0100549